NAQVI, S.R., NAQVI, M., INAYAT, A. and BLANCO-SANCHEZ, P. 2021. Impact of layered and delaminated zeolites on catalytic fast pyrolysis of microalgae using fixed-bed reactor and Py-GC/MS. *Journal of analytical and applied pyrolysis* [online], 155, article number 105025. Available from: https://doi.org/10.1016/j.jaap.2021.105025

Impact of layered and delaminated zeolites on catalytic fast pyrolysis of microalgae using fixed-bed reactor and Py-GC/MS.

NAQVI, S.R., NAQVI, M., INAYAT, A. and BLANCO-SANCHEZ, P.

2021

IMPACT OF LAYERED AND DELAMINATED ZEOLITES ON CATALYTIC FAST PYROLYSIS OF MICROALGAE USING FIXED-BED REACTOR AND PY-GC/MS

Salman Raza Naqvi[1*], Muhammad Naqvi[2], Abrar Inayat[3], Paula Blanco-Sanchez[4]
[1]School of Chemical & Materials Engineering, National University of Sciences & Technology, Islamabad, Pakistan; e-mail: salman.raza@scme.nust.edu.pk
[2]Department of Engineering and Chemical Sciences, Karlstad University, Karlstad 65188, Sweden; e-mail: raza.naqvi@kau.se
[3]Department of Sustainable and Renewable Energy Engineering, University of Sharjah, 27272, Sharjah, United Arab Emirates; e-mail: ainayat@sharjah.ac.ae
[4]Energy & Bioproducts Research Institute (EBRI), Aston University, B47ET, Birmingham, United Kingdom; e-mail: p.blanco-sanchez@aston.ac.uk

[*] Corresponding author: E-mail: salman.raza@scme.nust.edu.pk

Highlights

- In situ catalytic fast pyrolysis of BB was performed.
- ITQ-2 zeolite showed high deoxygenation capability.
- ITQ-2 zeolites produced more aromatic compounds as compared to MCM-22 zeolites.
- Pore structure and acidity of zeolites significantly impact on product composition.

Abstract

The aim of this work is to exploit the pyrolysis characteristics of microalgae *Botryococcus braunii* (BB) with a medium pore framework zeolite (MCM-22) and its delaminated counterpart with a higher external surface area zeolite (ITQ-2) using pyrolysis-gas-chromatography-mass-spectrometry (Py-GC/MS) and a fixed-bed reactor. The study evaluates the effect of synthesized zeolites that possess different pore size, shape and acidity on promoting deoxygenation reactions and producing aromatic compounds during the pyrolysis of microalgae. Further, the role of the shape of zeolites (layered & delaminated) for carbohydrate, protein and lipid-derived compounds formation is discussed. The Py-GC/MS results showed that the aromatic compounds (area%) was significantly higher (35.17 %) for delaminated & (28.76 %) for layered zeolites than non-catalytic pyrolysis (17.85%) at the catalyst/biomass ratio of 10.1. The increase in catalyst/biomass ratio from 3 to 10 at 550 °C has increased the aromatics (90.66 % for ITQ-2 & 75.25 %) for MCM-22 zeolites. In addition, ITQ-2 zeolite produced 20.47% higher aromatics than MCM-22 zeolites which is attributed to the thinner delaminated structure of ITQ-2 that makes reactants more accessible to the catalytic site and accelerate the deoxygenation reactions.

Keywords: Catalytic fast pyrolysis; zeolites; Microalgae; Py-GC/MS; Aromatics.

1. Introduction

Traditionally, fossil fuels have been the main source of energy to keep the modernization and development of life on earth. The rapid urbanization and escalated growth of population have substantially increased the energy demand and environmental issues due to the emissions linked to the use of fossil fuels [1-3]. The fuel security and environmental issues drove the world attention towards implementing Doha protocol and Paris climate change agreement to cut down the greenhouse gas emissions by developing and identifying alternative sources of energy [4, 5]. Biomass is considered as an alternative source of energy among other renewable sources due to its CO_2 neutrality, distributed availability around the globe, and sustainable life cycle [6-8]. The diverse spreads of biomass have its application for a variety of liquid and gaseous fuel productions such as biodiesel, syngas, methanol, methane etc. using various conversion technologies [9, 10].

Recently, microalgae is under consideration as a sources of energy by offering the advantages such as large productivity, ability to grow in diverse environment and weather conditions, no food and fuel crop competition, large content of natural lipids for biofuel production, and most importantly no use of urban land for its cultivation or growth [11, 12]. In spite of various advantages, the effective extraction of aromatic hydrocarbon or energy from algae pose many challenges such as long residence times, need of expensive catalyst and generation of waste streams [11]. For example microalgae have been used for the production of biodiesel through the transesterification process that requires longer residence time (1-4 h) and use of an expensive acidic catalyst [13]. In addition, only the lipids fraction of microalgae is used for biodiesel production process and the rest of algae component is considered as waste [12]. In order to address such challenges and issues, several researchers have continued to explore microalgae efficient conversion routes into the fuel that shall be commercially and economically viable [12]. Thermochemical and biochemical are the two promising technologies for biomass conversion into liquid, gas, and solid fuels [14]. Among thermochemical technologies, pyrolysis gained much attention because of biomass conversion into liquid fuels. The process is operated in the absence of air under the temperature range of 350 – 600 °C and produce products such as liquid, gases and biochar [15-17]. Hence, this technology can be utilized for microalgae conversion to valuable products. The conversion of microalgae into bio-oil through pyrolysis has many advantages such as the use of whole microalgae components and it yields a bio-oil with a higher heating value (HHV) and lower oxygen contents than bio-oil obtained from lignocellulosic organic material [18]. Microalgae-based bio-oil also has a significant amount of oxygen and nitrogen and large amount of components that significantly affect the quality of bio-oil in terms of stability and heating values [19].

The presence of oxygenates such as acids, ketones, aldehydes in the bio-oil may be reduced using catalysts during the biomass conversion via pyrolysis [20]. The catalysts can be used in-situ in the pyrolysis reactor or downstream in a separate catalytic reactor before vapours condensation, making it in-situ or ex-situ catalytic pyrolysis [21]. The use of zeolite-based catalysts in catalytic pyrolysis normally reduce the yield of bio-oil but improve its quality (in terms of composition and oxygen concentration). The use of zeolite catalyst and its combination with different transition metals such as nickel and gallium could enhance the yield of aromatics in the bio-oil by accelerating the decarboxylation, dehydration, decarbonylation, and aromatization reactions [18].

Out of many studies on the catalytic pyrolysis of algal-based biomass pyrolysis process using commercial zeolites, very few have reported studying the influence of the pore size and shape of selective synthesized zeolites [22]. For example, Du et al., 2013 used three type of commercial zeolite- based catalysts: H-Y, H-Beta and H-ZSM5 for the catalytic pyrolysis of microalgae in a pyroprobe system [18]. His studies showed the highest aromatics yield of 18.13 vol% for the catalytic pyrolysis of microalgae with H-ZSM5. The algal biomass has a different composition than lignocellulosic biomass as it mostly consists of three major components namely carbohydrates, lipids, and proteins. In terms of aromatics yield in the bio-oil, it is therefore important to study the effect of catalyst on these components during pyrolysis process. In another report, Du et al., 2013 investigated the effect of a zeolite-based catalyst on these components during pyrolysis and reported that most of the aromatics are obtained by the conversion of lipids and carbohydrates while proteins contribute into a lesser degree [11]. The contributions from these microalgae components towards hydrocarbon formation have been also reported in the literature for different types of microalgae. For example Azizi et al, 2017 studied the pyrolysis kinetics of *Chlorella vulgaris* showed that the interaction is inhibitive than synergistic during the decomposition process [23]. Furthermore, Ji et al, 2017 investigated the co-pyrolysis of bamboo with microalgae and observed 66 wt.% of bio-oil yield [24]. In a recent study, the catalytic pyrolysis of an aquatic biomass, (*Tribonema minus)*, was performed over the Ni-MgO/HZSM-5 catalyst in order to investigate the effect of catalyst on products yields and composition. It was reported that the addition of the MgO promoter to Ni/HZSM-5 contributed to the inhibition of coke formation, decrease the acids and esters, and an increase of the hydrocarbons fraction [24]. Considering these reports, the pyrolysis of microalgae to produce aromatic compounds in an efficient manner needs further investigation. For example, it is important to study the role of different types of catalysts together with different catalyst: biomass ratios on the quantity and the quality of bio-oil. Microalgae can be classified into carbohydrate, protein and lipids. BB microalgae fall in an important class of microalgae that shows high carbohydrate and lipid contents. The aim of this study is to investigate the effect of the shape of selective synthesized zeolites on the pyrolysis conversion of high carbohydrate and lipid microalgae (BB) into aromatics. According to authors' best knowledge; very few studies have reported such algae specie who has high protein and carbohydrate content in fast pyrolysis process for aromatics production. The study developed and applied layered and delaminated zeolites which possessed different pore size (10-12 MR), shape (layered & delaminated) and acidity (low and high) to promote deoxygenation reactions and could enhance aromatics production.

2. Materials and methods

2.1 Preparation of algal biomass

The initial stock of *Botryococcus braunii* was purchased from Algaetech International Sdn. Bhd. (Malaysia). The inoculum was first precultured in Blue Green (BG-11) growth medium which composed of distilled water and the following chemical ingredients; $NaNO_3$ 1.5 g L^{-1}, K_2HPO_4 0.04 g/L, $MgSO_4.7H_2O$ 0.075 g L^{-1}, $CaCl_2.2H_2O$ 0.036 g L^{-1}, $C_6H_8O_7.H_2O$ 0.006 g L^{-1}, Ferric citrate 0.006 g L^{-1}, EDTA-Na_2 0.001 g L^{-1}, Na_2CO_3 0.020 g L^{-1}, H_3BO_3 2.86x10^{-3} g L^{-1}, $MnCl_2.4H_2O$ 1.81x 10-3 g L^{-1}, $ZnSO_4.7H_2O$ 0.222 x 10^{-3} g L^{-1}, $NaMoO_4.2H_2O$ 0.390x 10^{-3} g L^{-1}, $CuSO_4.5H_2O$ 0.079x 10^{-3} g L^{-1}, $Co(NO_3)_2.6H_20$ 0.049x10^{-3} g L^{-1}. Then the pH was adjusted to 7.11 by using 0.1M citric acid. The culture was kept at 25±2 °C for 10 d with continuous light supplied by white-fluorescent tubes. The culture was also put under aeration at a flow rate of 2 L min^{-1} for 5 L working volume. An aliquot (20 mL) of each algal solution was centrifuged at 3500 rpm for 10 min using HERMLE centrifuge. Then the sample was dried in the drying oven at 105 °C for 48 h.

2.2 Characterization of algae

The physicochemical properties of *B. braunii* (BB) are shown in Table 1. Proximate analysis (moisture, ash, volatiles and fixed carbon) of the algae was carried out using ASTM standards reported in one of authors' previous publication [25]; whereas the ultimate analysis (C, H, N, and O) was carried out in an Elemental analyzer (VarioMicro CHNS analyzer). The chemical composition (carbohydrate, protein, and lipids) of the microalgae was determined by following the reported methods [26, 27]. A bomb calorimetry (Model-IKA C2000) was used to determine the higher heating value (HHV) of the microalgae. To exploit the thermal decomposition profile of BB, weight loss and derivative weight loss curves were generated using a thermogravimetric analyzer (Q50, TA instrument). Between 5 - 6 mg of BB sample was heated from 292 K to 1170 K at a heating rate of 10°C min^{-1} and with a nitrogen flow rate of 60 ml min^{-1}.

2.3 Catalysts

The synthesis and characterization details of layered (MCM-22) and delaminated zeolites (ITQ-2) with a Si/Al = 35 ratio is already reported in our previous publication [28]. Zeolites were calcined to their active hydrogen form at 550 °C in air for 5 h. In our previous study, both zeolites showed deoxygenation of lignocellulosic biomass pyrolysis vapors and this was the first study in which the impact of zeolites shape selectivity on a high carbohydrate and proteinaceous biomass was demonstrated. The porous structure of layered and delaminated zeolites were measured by N_2 adsorption/desorption at 77.15 K on a Micrometrics ASAP 2010 instrument.

2.4 Fixed-bed pyrolyzer

Non-catalytic and catalytic fast pyrolysis experiments were performed using a fixed-bed drop type pyrolyzer. The cylindrical reactor was featured with 53 mm internal diameter and 155 mm in height and it was connected to a vacuum and nitrogen gas lines to generate inert conditions throughout the setup. A determined amount of biomass was kept in a holder zone between the two ball values and dropped into the reaction zone after achieving the required temperatures such as 450, 500 and 550 °C. The temperature inside the reaction zone was recorded using a L-type thermocouple. The heating rate of the fixed-bed pyrolyzer was adjusted around 1000 °C min^{-1}. Around 10 g of biomass was mixed with catalyst (in-bed mode) and pyrolyzed in the reactor at 500 °C with variable catalyst/biomass loadings of 3:1, 5:1 and 10:1. The pyrolysis vapors were condensed and collected in two series condensers which were connected to a cooled ethylene glycol bath below – 10 °C. The pyrolysis oil was consisted of organics oil and water phase. The yields of the liquid, solid and gaseous resulting fractions, were determined as follows. The fraction of liquid was calculated by dividing the mass of collected bio-oil to the mass the biomass. The residual solid yield inside the reactor was obtained as the residual solid mass divided by the mass of biomass. The yield of gas was calculated by applying overall material balance. The experiments were done in triplicate for data precision and to determine any experimental error. Figure 1 depicts the schematic diagram of the drop type fixed-bed reactor. Non-condensable gases are characterized using a GC (GC-8A, Shimadzu Co., Ltd) equipped with a thermal conductivity detector. The water content of the produced bio-oil was determined using Karl Fisher titrator (Metrhom 787 KF Titrino).

2.5 Py-GC/MS

Fast pyrolysis experiments were performed in a single shot micropyrolyzer (PY-3030S, Frontier Laboratories, Japan) and the products were analyzed in a GC/MS (Shimadzu GC-2010 and QP2010). The analytes were separated in a UA-5 column (30 m length × 0.25 mm internal diameter × 0.25 m thickness, stationary phase: 5% diphenyl dimethyl polysiloxane). Algae samples of c.a. 3 mg were taken in a deactivated stainless-steel cup and dropped into the quartz tube that was surrounded by the micro-pyrolyzer furnace. The furnace was pre-calibrated to read the centerline temperature of the tube. The pyrolysis temperature was set in the range of 450–550 °C. For catalytic fast pyrolysis experiments, the calculated amounts of algae and catalyst were thoroughly mixed in a mortar and taken in the sample cup. Experiments were performed in helium (99.99% purity) environment. Helium flow rate through the column was set at 2 mL min^{-1} with a split ratio of 100:1. Prior to dropping the sample cup inside the quartz tube, helium was purged for a few minutes. GC column oven was held at 40 °C for 1 min, then heated at a rate of 20 °C min^{-1} to 300 °C, and finally held at 300 °C for 30 min. MS ion source temperature was maintained at 300 °C, and all the pyrolysis products were scanned in a mass range (m/z) of 28–300 Da. The products were confirmed by comparing their mass spectra with NIST mass spectral database for a high (>80%) percentage match. The relative composition of the various organic compounds in the pyrolysate was calculated as area% under the GC/MS peak. Most of the non-catalytic and catalytic fast pyrolysis experiments were repeated three times. The standard deviation in area% of the GC/MS peaks for the various products was found to be <5%.

3. Results and discussion

3.1 Characterization of algae and catalysts

The moisture, volatile matter, fixed carbon and ash content of *Spirulina* algae were 3.5%, 76.1%, 17.9% and 2.4% respectively. The C, H, N, S and O composition was 51.5%, 8.9%, 7.5% and 32.1%, respectively. BB microalgae possessed high volatiles and carbon content as compared to *Spirulina* and *Nannochloropsis sp*. microalgae as shown in Table 1. Based on the growth conditions, the BB microalgae has a high carbohydrate (24.39 %), comparable protein (34.0%) and high lipid content (20.2%) as compared to *Scenedesmus dimorphus* and *Spirulina* microalgae (Table 1). In comparison to lignocellulosic biomasses that contain <2.5% nitrogen [28], BB is rich in nitrogen due to the high content of proteins. The HHV of the algae sample was 21.5 MJ kg^{-1}.

Two shape selective zeolites, (i) layered zeolites, MCM-22 and (ii) its delaminated counterpart, ITQ-2, synthesized and employed in high carbohydrate and lipids-derived microalgae. Briefly, layered and delaminated zeolites belong to MWW class of zeolites. MWW zeolites structure contains two independent pore systems. One system is defined by 10-MR channel with dimensions of (4.0 x 5.5 Å) and another system consists of supercages delaminated by 12-MR channel with a dimension of (7.1 x 7.1 x 18.1 Å). These supercages are connected through 10-MR window with a dimension of (4.1 x 5.1 Å). The BET surface area of layered zeolites and its delaminated counterpart are 226 and 546 (m^2 g^{-1}) respectively. Delaminated zeolites possess a higher external surface area (442 m^2 g^{-1}) than layered zeolites (100 m^2 g^{-1}). In terms of acidity and total acid active sites as shown in a previous study following the order as: delaminated zeolites > layered zeolite [28].

3.2 Thermal analysis of algae

Figure 2 shows the thermogravimetric characteristics of *B. braunii* when heated from 18.8 °C to 896.8 °C at 10 °C min^{-1}. Two main regions of the weight loss can be identified from the figure.

Zone 1 (126.8 – 576.8 °C), is an active pyrolysis zone where major weight loss occurs with a peak-maximum temperature of 313.3 °C. It is during this temperature range, the main constituents of the algae undergo thermal cracking [18]. At the end of the active pyrolysis zone, the mass loss reaches to a substantial 77.10%. After zone 1, the weight loss continues but at a very low rate. In this zone, the trapped volatiles normally escape with least thermal decomposition. It is also worth noting here that the active pyrolysis zone (temperature range of 126.8 – 576.8 °C) contains overlapping peaks, which corresponds to the degradation of the microalgae constituents. For *B. braunii,* the main constituents are carbohydrates, proteins, and lipids. Carbohydrates usually degrade in the temperature range of 199.8 – 349.8 °C [29] whereas the degradation of protein takes place in the narrow temperature range of 219.8 – 300.8 °C [30, 31]. Lipids, compared to carbohydrates and proteins, thermally degrade at relatively higher temperatures (269.8 – 579.8 °C) [32].

3.3 Pyrolysis products yield

Few studies in literature showed the optimum temperature of pyrolysis oil production from microalgae [33, 34]. Products (gas, organics oil, water and solid char) yield at various pyrolysis temperatures (450, 500 and 550 °C) in the absence of a catalyst is presented in Figure 3. The results showed that temperature has a significant impact on the production of water and gas production. In terms of char, the yield is decreased (44.67 - 36.28 wt.%) with the increase of temperature. This finding is in good agreement with the thermogravimetric data which shows that at a temperature of 126.8 – 576.8 °C for the decomposition of *B. braunii*. On the other hand, gas yield showed opposite trend and increased (24.11 - 32.27 wt.%) with the increase of temperature. Similar observation is reported in the literature and described as due to various extents of secondary reactions [35]. In terms of pyrolysis oil (organics + water), the yield is reached at its maximum (31.68 wt.%) at 500 °C. Beyond this temperature (i.e. at 550 °C), the yield of pyrolysis oil started decreasing because of secondary cracking of pyrolysis vapors. Yuan et al, 2015 studied pyrolysis characteristics of *C. vulgaris* in a fixed-bed reactor at various temperatures [36]. Their results showed similar trends of oil, gas and char yields to those reported in this work. In another study conducted by Pan et al, 2010 on *Nannochloropsis sp.* algae in a fixed-bed reactor during non-catalytic pyrolysis, the temperature showed a significant impact on products yield and depicted similar trends [33].

Based on the oil yield results of non-catalytic pyrolysis experiments, 500 °C is chosen for catalytic pyrolysis experiments. The products yield of non-catalytic and catalytic pyrolysis (various catalyst/biomass ratios) is presented in Figure 3. It can be deduced from the results; oil yield is decreased substantially by employing catalyst in various ratios as compared to non-catalytic pyrolysis process. This happened by enhancing secondary cracking due to the catalyst acidity and diffusion into pore size which facilitates reploymerization and aromatization to occur. For example, the increased gas and water formation are due to deoxygenation reactions such as dehydration, decarbonylation and decarboxylation [37]. Among catalysts, layered zeolite showed water and gas yields of 17.45-19.38 wt.% and 33.22- 35.40 wt.% in comparison to non-catalytic 18.99 and 28.98 wt.%, respectively. From Figure 3b, it is observed that the organics content is decreased (10.22 - 6.21 wt.%) by increasing catalytic loadings from 3:1 up to 10:1 for MCM-22 catalyst. However, it is worth noticing that delaminated structured deoxygenates remarkably and showed water and gas yields of 18.01- 20.05 wt.% and 34.66- 36.02 wt.% by increasing catalytic amounts from 3:1 up to 10:1 for ITQ-2 catalyst. In our previous study, thin sheets of delaminated zeolites showed mild mesoporousity at the external surface area which benefits higher catalytic activity [38]. It can be deduced from these results that volatiles released during pyrolysis interact on the surface and pore geometry of the catalyst at which active acid sites are present and promote secondary cracking such as decarbonylation, decarboxylation, release of water and increase gas contents. Similar observations are reported by for the pyrolysis of *Chlorella vulgaris* over Ni supported zeolite catalyst [39].

3.4 Product gas composition

The third component of pyrolysis products is product gases consisting of H_2, CO, CO_2 and CH_4. Figure 4 shows the composition of product gases without catalyst and using catalyst MCM-22 (35) and ITQ-2 (35) at 500 °C by varying the catalyst/biomass ratios (3:1, 5:1, 10:1). It is clear from Figure 4 that the overall gas production is increased with the use of catalyst. From Figure 4, it can observed that the production of both CO and CO_2 is higher when using ITQ-2 zeolites as compared to H_2 and CH_4 for all cases. The second information can be drawn that H_2 and CH_4 composition is higher in case of MCM-22 zeolites cracking. On the other hand, ITQ-2 zeolites appeared as promising catalyst for effective deoxygenation reactions.

3.5 Non-catalytic Py-GC/MS

Non-catalytic fast pyrolysis experiments of *B. braunii* were conducted at three pyrolysis temperature of 450, 500 and 550 °C. All experiments were performed in triplicate. Figure 5 shows the production of main chemical compounds (area %) present in the non-catalytic pyrolysis of *B. braunii* at 450, 500 and 550 °C. The main chemical compounds identified were; alkanes and alkenes, carboxylic acid, alcohols, esters, nitriles, N-containing compounds, monoaromatics, cyclic organic compounds and naphthenic compounds. The results showed that the production of compounds are influenced by temperature. The amounts of compounds (alkanes & alkenes, alcohols, nitriles, N-containing compounds, monoaromatics and cyclic organic compounds) increased with the increase in temperature. On the other hand, carboxylic acids and esters showed a decreasing trend with the increase of temperature. Hence, the decreasing order of the compounds with respect to their content was: carboxylic acids > monoaromatics > N-containing compounds > alcohols > alkanes & alkenes > naphthenic compounds > esters > cyclic organic compounds > nitriles. *B. braunii* microalgae showed reasonable carbohydrate content and this lead to carboxylic acids, furans and anhydrosugars production in bio-oil produced from carbohydrate-derived compounds [40, 41]. Zainan et al. observed large quantities of oxygenated compounds and N-containing compounds from non-catalytic pyrolysis of *T. suecica* at the temperature range of 300 – 600 °C [42]. According to chemical composition data, *B. braunii* possessed high protein content. It is evident that production of aromatic hydrocarbon, N-containing compounds, and nitriles from high protein-derived compounds increase at a high pyrolysis temperature [43]. Du et al investigated the pyrolysis-GC/MS of *C. vulgaris* microalgae, Cellulose, Egg whites, Canola oil over the pyrolysis temperature range of 450-600 °C [11]. The study concluded that aromatic hydrocarbon were the protein-derived fractions. Hydrocarbons (monoaromatics, cyclic organic compounds, and naphthenic compounds) were protein and lipids-derived compounds and their content increased with the increase of temperature.

Another important aspect is the secondary pyrolysis oil reactions in the vapor phase at high temperatures (>500 °C) which produce more aromatics and light gases (Figure 5). These observations are well in agreement with the literature [44].

3.6 Catalytic Py-GC/MS

The aim of this study is to exploit the impact of catalyst on deoxygenation of high protein and low lipid-derived compounds. Two shape selective zeolites; (1) layered (MCM-22 with Si/Al ratio of 35) and (2) delaminated zeolites (ITQ-2 with Si/Al ratio of 35) were tested in Py-GC/MS. The compounds with particular interest (aromatic hydrocarbons) and effect of both catalysts loading is important since the compounds are related to protein and lipids-derived compounds. Therefore, it was the reason; the pyrolysis temperature of 550 °C was selected for the catalytic pyrolysis of *B. braunii*.

3.6.1 Effect of layered zeolites

The catalytic pyrolysis of layered zeolite (MCM-22) with various catalysts/BB loadings (3:1, 5:1, 10:1) were employed in Py-GC/MS at 550 °C. The results of various compounds (area %) produced in comparison to non-catalytic and catalytic pyrolysis of *B. braunii* are shown in Figure 6. In comparison to non-catalyst, layered zeolite catalyst reduced the formation of oxygenated species (carboxylic acid, alcohols, esters and N-containing compounds) Figure 5. The pore size, shape and acidity of microporous zeolite catalysts claimed high activity and responsible for high deoxygenation [28]. The layered type zeolite impacts the deoxygenation of carbohydrate-derived compounds and promotes the formation of desirable components.

Interestingly, the amount of nitriles increased as the layered zeolite loading increased. At catalysts/BB ratio (10:1), 3.25 (area %) of nitriles produced in comparison to non-catalytic pyrolysis of *B. braunii* (0.9%). This might imply cracking of long chain portion of nitriles. As the catalyst loading increased, the formation of N-containing compounds showed rapid decrement. It is due to secondary cracking of protein-derived components. By increasing the catalyst amount, more monoaromatics, cyclic organic compounds, and naphthenic compounds were produced. This finding fits well with the catalytic pyrolysis of lignocellulosic molecules which show deoxygenation and produce aromatics on commercial zeolite (e.g. HZSM-5) [45, 46]. Based on this study, it is evident that layered zeolite provides enough surface (microporous + external surface area) to crack carbohydrate-derived components and promotes secondary cracking of protein-derived components to produce aromatic hydrocarbons and naphthenic compounds. This layered material might possess a higher concentration of Bronsted acid sites which deoxygenates sugar and carboxylic acid molecules and produce aromatic hydrocarbons.

The catalyst and their increased amount cracked large N-containing compounds and produced cyclic organic compounds and naphthenic compounds.

3.6.2 Effect of delaminated zeolites

The delaminated counterpart, ITQ-2 zeolite catalyst is mixed with the microalgae to exploit the effect of the physical structure of zeolites on proteinaceous biomass pyrolysis. These results provide an opportunity to draw the performance comparison between layered and delaminated zeolites to selectively produce aromatic and naphthenic compounds formation on protein and lipid-derived compounds. Figure 7 represents the non-catalytic and catalytic pyrolysis of microalgae at various catalyst/biomass ratios (3:1, 5:1, 10:1) in Py-GC/MS at 550 °C. From Figure 7 it is observed that there was a drastic decrease in oxygenated species compared to non-catalytic and layered zeolites. As the catalyst/biomass ratio increases, the amount of carboxylic acid, alcohols, esters and N-containing compounds decrease significantly. On the other hand, the oxygenated compounds cracked on the inner and external active surface of the delaminated counterpart zeolites and enhanced the formation of aromatic and naphthenic compounds. Importantly, the alcohols and carboxylic acid were substantially lowered by employing delaminated zeolites, ITQ-2.

Compared to non-catalyst and layered zeolite at low catalyst/biomass ratio (3:1), delaminated zeolites were superior for the production of alkanes & alkenes than alcohols, acids and ester. It was noted that increasing the catalyst loading resulted in an increase of alkane by cracking of long-chain compounds. Besides this, nitriles production increased and N-containing compounds decreased with the increase of the catalyst/biomass ratio of 3:1 to 10:1. This might be due to the unique framework of the delaminated counterpart. The addition of delaminated zeolites led to the higher production of monoaromatics, cyclic and naphthenic compounds in comparison to non-catalyst and layered zeolites. The total hydrocarbon contents (monoaromatic + cyclic + naphthenic) at lower catalyst/biomass ratio (3:1) was higher using delaminated zeolites (25.4%) as compared to layered zeolite (21.5%) and non-catalyst (17.8%). At higher catalyst/biomass loading, (10:1), the total hydrocarbon content was much higher using delaminated zeolites (35.1%) than layered zeolite (28.7%) and non-catalyst (17.8%). Unique physical structure of zeolites with high acidity promoted cracking of large chain molecules on more accessible active sites. This caused not only faster transport from catalytic site to the bulk but also decreased the secondary cracking to form gases synthesized alkyl 5-benzyl-2-furoates as intermediates for fine chemicals using two-dimensional delaminated ITQ-2 zeolite [20, 47, 48]. Their results concluded that ITQ-2 zeolite was the active and selective catalyst to produce alkyl 5-benzyl-2-furoates which combines easy product diffusion and adequate acidity [49]. Overall, this study is in good agreement with the literature and elucidates the impact of catalyst to deoxygenate the oxygenated components and enhance aromatic compounds.

4. Conclusions

Non-catalytic and catalytic pyrolysis investigation of *B. braunii* is studied using fixed-bed pyrolyzer and Py-GC/MS analysis. The layered zeolite catalysts (MCM-22 with Si/Al ratio of 35) reduce the formation of oxygenated species (carboxylic acids, alcohols, esters and N-compounds) as compared to non-catalytic pyrolysis. Furthermore, the delaminated zeolites are better for alkanes and alkenes production with low alcohol, acids, and ester formation. In addition, total content of monoaromatics, cyclic and napthenic compounds is found to be higher at lower catalyst/biomass ratio (3:1) using delaminated zeolites (25.4%) as compared to layered zeolite (21.5%) and non-catalyst (17.8%). ITQ-2 zeolite is more active and shape selective catalyst which combine easy product diffusion and adequate acidity to produce monoaromatics and naphthenic compounds.

Credit author statement;
Salman Raza Naqvi (Conceptualization, Investigation, Writing-original draft, Funding acquisition, Supervision), M. Naqvi (Methodology, Writing-Review & Editing), Abrar Inayat (Project Management, Writing-review & editing), Paula Blanco-Sanchez (Validation, Formal Analysis, Writing-Review & Editing)

Declaration of interests

The authors declare that they have no known competing financial interests or personal relationships that could have appeared to influence the work reported in this paper.

Acknowledgements

The author would also like to acknowledge the National University of Science and Technology (NUST) Pakistan. The corresponding author would like to acknowledge Kurita Water and Environment Foundation, grant number 20P006-14 for financial support.

References

1. Beig, B., et al., *Current challenges and innovative developments in pretreatment of lignocellulosic residues for biofuel production: A review.* 2020: p. 119670.
2. Dai, L., et al., *Recent advances in improving lignocellulosic biomass-based bio-oil production.* 2020: p. 104845.
3. Naqvi, S.R., et al., *New trends in improving gasoline quality and octane through naphtha isomerization: a short review.* 2018. **8**(3): p. 131-139.
4. Shahbaz, M., et al., *Optimization of hydrogen and syngas production from PKS gasification by using coal bottom ash.* Bioresource Technology, 2017. **241**: p. 284-295.
5. Naqvi, M., et al., *Waste biomass gasification based off-grid electricity generation: a case study in Pakistan.* 2016. **103**(103): p. 406-412.
6. Naqvi, S.R.J.S.P.S., *RECENT DEVELOPMENTS ON BIOMASS UTILIZATION FOR BIOENERGY PRODUCTION IN PAKISTAN.* 2020. **2**(2): p. 156-160.
7. Cheng, F., et al., *Impact of feedstock composition on pyrolysis of low-cost, protein-and lignin-rich biomass: A review.* 2020. **147**: p. 104780.
8. Naqvi, S.R., et al., *Assessment of agro-industrial residues for bioenergy potential by investigating thermo-kinetic behavior in a slow pyrolysis process.* 2020. **278**: p. 118259.
9. Pang, Y.X., et al., *The Influence of Lignocellulose on Biomass Pyrolysis Product Distribution and Economics via Steady State Process Simulation.* 2020: p. 104968.
10. Paysepar, H., et al., *Production of phenolic chemicals from hydrolysis lignin via catalytic fast pyrolysis.* 2020: p. 104842.
11. Du, Z., et al., *Catalytic pyrolysis of microalgae and their three major components: Carbohydrates, proteins, and lipids.* Bioresource Technology, 2013. **130**(Supplement C): p. 777-782.
12. Wang, K. and R.C. Brown, *Catalytic pyrolysis of microalgae for production of aromatics and ammonia.* Green Chemistry, 2013. **15**(3): p. 675-681.
13. Ehimen, E., Z. Sun, and C. Carrington, *Variables affecting the in situ transesterification of microalgae lipids.* Fuel, 2010. **89**(3): p. 677-684.
14. Materazzi, M. and A. Holt, *Experimental analysis and preliminary assessment of an integrated thermochemical process for production of low-molecular weight biofuels from municipal solid waste (MSW).* Renewable Energy, 2019. **143**: p. 663-678.
15. Ly, H.V., et al., *Catalytic pyrolysis of bamboo in a bubbling fluidized-bed reactor with two different catalysts: HZSM-5 and red mud for upgrading bio-oil.* Renewable Energy, 2020. **149**: p. 1434-1445.
16. Hameed, Z., et al., *Kinetic and thermodynamic analyses of sugar cane bagasse and sewage sludge co-pyrolysis process.* 2018. **32**(9): p. 9551-9558.
17. Naqvi, S.R., et al., *Catalytic pyrolysis of paddy husk in a drop type pyrolyzer for bio-oil production: The role of temperature and catalyst.* 2014. **106**: p. 57-62.
18. Du, Z., et al., *Production of aromatic hydrocarbons by catalytic pyrolysis of microalgae with zeolites: Catalyst screening in a pyroprobe.* Bioresource Technology, 2013. **139**(Supplement C): p. 397-401.
19. Thangalazhy-Gopakumar, S., et al., *Catalytic pyrolysis of green algae for hydrocarbon production using H+ZSM-5 catalyst.* Bioresource Technology, 2012. **118**: p. 150-157.
20. Hu, S., et al., *Experimental study and economic feasibility analysis on the production of bio-oil by catalytic cracking of three kinds of microalgae.* 2020: p. 104835.
21. Güngör, A., et al., *Comparison between the "one-step" and "two-step" catalytic pyrolysis of pine bark.* Journal of analytical and applied pyrolysis, 2012. **97**: p. 39-48.

22. Fermoso, J., et al., *11 - Pyrolysis of microalgae for fuel production A2 - Gonzalez-Fernandez, Cristina*, in *Microalgae-Based Biofuels and Bioproducts*, R. Muñoz, Editor. 2017, Woodhead Publishing. p. 259-281.
23. Azizi, K., M.K. Moraveji, and H.A. Najafabadi, *Characteristics and kinetics study of simultaneous pyrolysis of microalgae Chlorella vulgaris, wood and polypropylene through TGA.* Bioresource technology, 2017. **243**: p. 481-491.
24. Ji, X., et al., *Effect of MgO promoter on Ni-Mg/ZSM-5 catalysts for catalytic pyrolysis of lipid-extracted residue of Tribonema minus.* Journal of Analytical and Applied Pyrolysis, 2017. **123**: p. 278-283.
25. Naqvi, S.R., Y. Uemura, and S.B. Yusup, *Catalytic pyrolysis of paddy husk in a drop type pyrolyzer for bio-oil production: The role of temperature and catalyst.* Journal of Analytical and Applied Pyrolysis, 2014. **106**: p. 57-62.
26. Bianchini, E., et al., *Pyrolysis of spirulina and zeolite cracking over HZSM-5. An analytical investigation on the chemical route of bio-oil from cultivation to combustion.* Journal of Analytical and Applied Pyrolysis, 2017. **126**: p. 230-238.
27. Bordoloi, N., et al., *Characterization of bio-oil and its sub-fractions from pyrolysis of Scenedesmus dimorphus.* Renewable Energy, 2016. **98**: p. 245-253.
28. Naqvi, S.R., et al., *In situ catalytic fast pyrolysis of paddy husk pyrolysis vapors over MCM-22 and ITQ-2 zeolites.* Journal of Analytical and Applied Pyrolysis, 2015.
29. Pavlath, A.E. and K.S. Gregorski, *Atmospheric pyrolysis of carbohydrates with thermogravimetric and mass spectrometric analyses.* Journal of Analytical and Applied Pyrolysis, 1985. **8**: p. 41-48.
30. Dandurand, J., et al., *Conformational and thermal characterization of a synthetic peptidic fragment inspired from human tropoelastin: Signature of the amyloid fibers.* Pathologie Biologie, 2014. **62**(2): p. 100-107.
31. Samouillan, V., et al., *Thermal analysis characterization of aortic tissues for cardiac valve bioprostheses.* Journal of biomedical materials research, 1999. **46**(4): p. 531-538.
32. Muniz, M.A.P., et al., *Physicochemical characterization, fatty acid composition, and thermal analysis of Bertholletia excelsa HBK oil.* Pharmacognosy magazine, 2015. **11**(41): p. 147.
33. Pan, P., et al., *The direct pyrolysis and catalytic pyrolysis of Nannochloropsis sp. residue for renewable bio-oils.* Bioresource Technology, 2010. **101**(12): p. 4593-4599.
34. Li, R., et al., *Selection of temperature for bio-oil production from pyrolysis of algae from lake blooms.* Energy and Fuels, 2012. **26**(5): p. 2996-3002.
35. Kersten, S.R.A., et al., *Options for Catalysis in the Thermochemical Conversion of Biomass into Fuels*, in *Catalysis for Renewables: From Feedstock to Energy Production*. 2007. p. 119-145.
36. Yuan, T., A. Tahmasebi, and J. Yu, *Comparative study on pyrolysis of lignocellulosic and algal biomass using a thermogravimetric and a fixed-bed reactor.* Bioresource Technology, 2015. **175**: p. 333-341.
37. Thangalazhy-Gopakumar, S., et al., *Catalytic pyrolysis of green algae for hydrocarbon production using H+ZSM-5 catalyst.* Bioresource Technology, 2012. **118**: p. 150-157.
38. Naqvi, S.R., et al., *In situ catalytic fast pyrolysis of paddy husk pyrolysis vapors over MCM-22 and ITQ-2 zeolites.* Journal of Analytical and Applied Pyrolysis, 2015. **114**: p. 32-39.
39. Zainan, N.H., et al., *Quality of bio-oil from catalytic pyrolysis of microalgae Chlorella vulgaris.* Fuel, 2018. **223**: p. 12-19.
40. Stevens, C. and R.C. Brown, *Thermochemical processing of biomass: conversion into fuels, chemicals and power*. 2011: John Wiley & Sons.
41. Mohan, D., C.U. Pittman, and P.H. Steele, *Pyrolysis of wood/biomass for bio-oil: a critical review.* Energy & fuels, 2006. **20**(3): p. 848-889.

42. Zainan, N.H., S.C. Srivatsa, and S. Bhattacharya, *Catalytic pyrolysis of microalgae Tetraselmis suecica and characterization study using in situ Synchrotron-based Infrared Microscopy.* Fuel, 2015. **161**: p. 345-354.
43. Wang, K., et al., *Fast pyrolysis of microalgae remnants in a fluidized bed reactor for bio-oil and biochar production.* Bioresource technology, 2013. **127**: p. 494-499.
44. Gilbert, P., et al., *Tar reduction in pyrolysis vapours from biomass over a hot char bed.* Bioresource Technology, 2009. **100**(23): p. 6045-6051.
45. Mihalcik, D.J., C.A. Mullen, and A.A. Boateng, *Screening acidic zeolites for catalytic fast pyrolysis of biomass and its components.* Journal of Analytical and Applied Pyrolysis, 2011. **92**(1): p. 224-232.
46. Mullen, C.A. and A.A. Boateng, *Catalytic pyrolysis-GC/MS of lignin from several sources.* Fuel Processing Technology, 2010. **91**(11): p. 1446-1458.
47. Arias, K.S., et al., *Two-Dimensional ITQ-2 Zeolite for Biomass Transformation: Synthesis of Alkyl 5-Benzyl-2-furoates as Intermediates for Fine Chemicals.* ACS Sustainable Chemistry & Engineering, 2016. **4**(11): p. 6152-6159.
48. Naqvi, S.R., et al., *Catalytic pyrolysis of Botryococcus Braunii (microalgae) over layered and delaminated zeolites for aromatic hydrocarbon production.* 2017. **142**: p. 381-385.
49. Naqvi, S.R., et al., *Catalytic consequences of micropore topology on biomass pyrolysis vapors over shape selective zeolites.* 2017. **105**: p. 557-561.

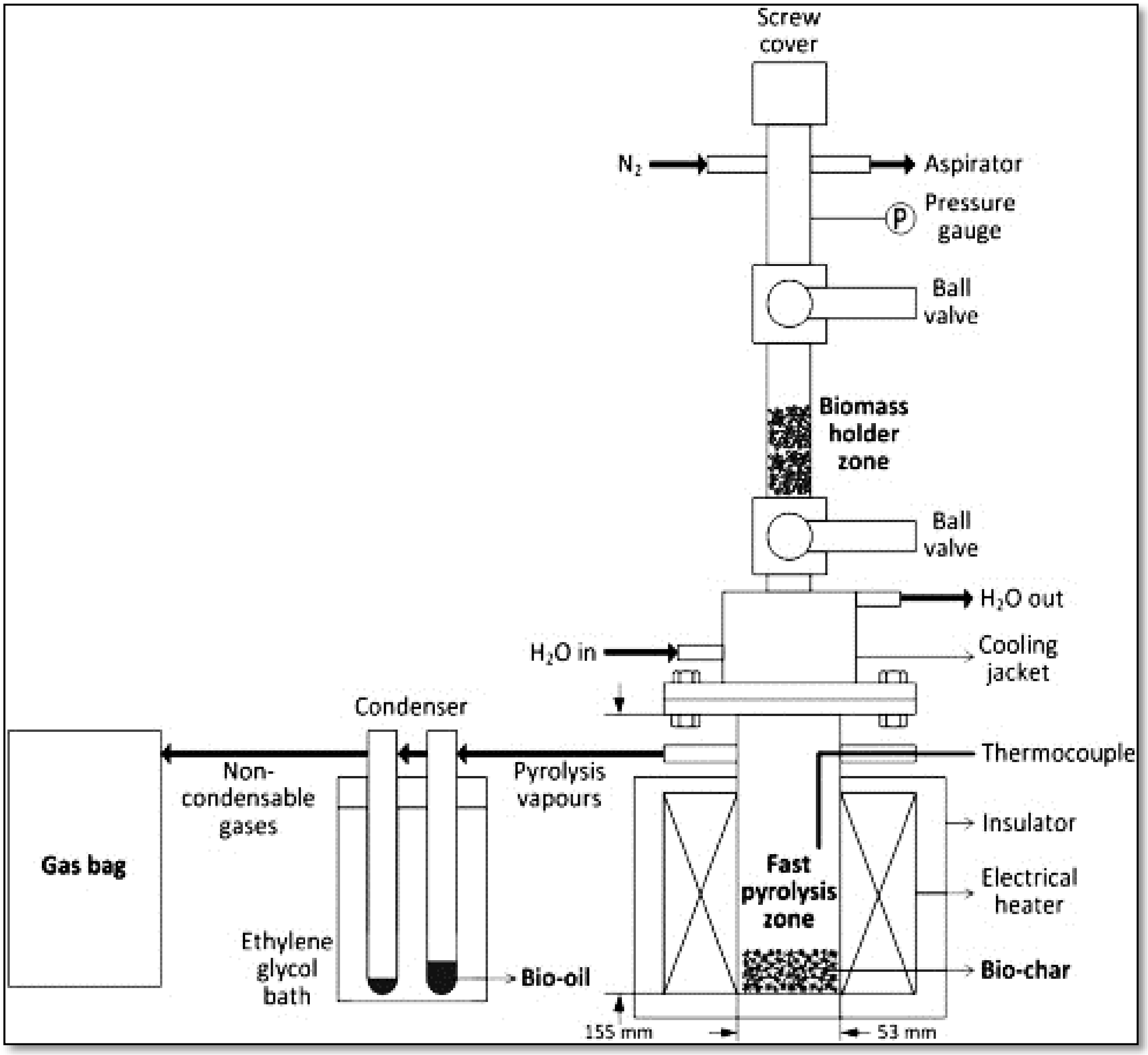

Figure 1: Schematic diagram of the drop type fixed-bed reactor.

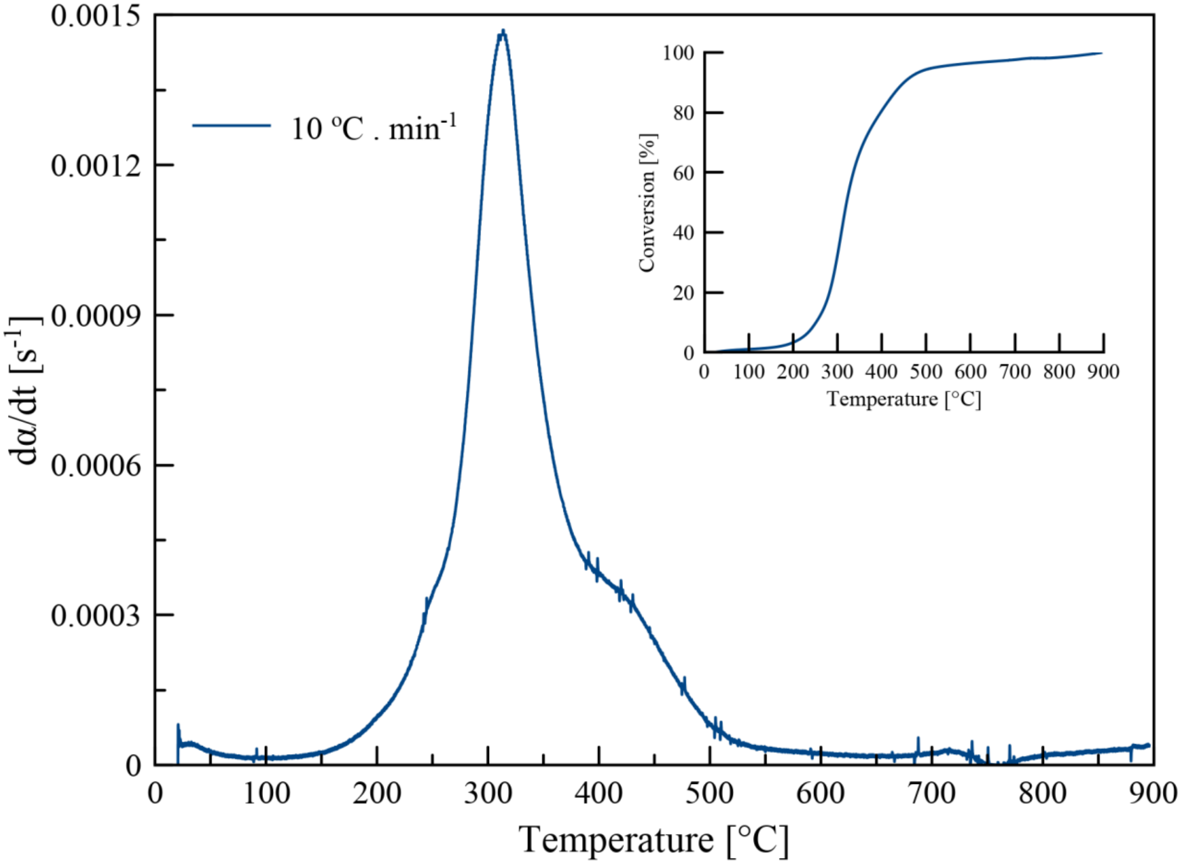

Figure 2: Thermogravimetric mass loss (TG) and differential mass loss (DTG) curves for *B. braunii* at 10 °C/min.

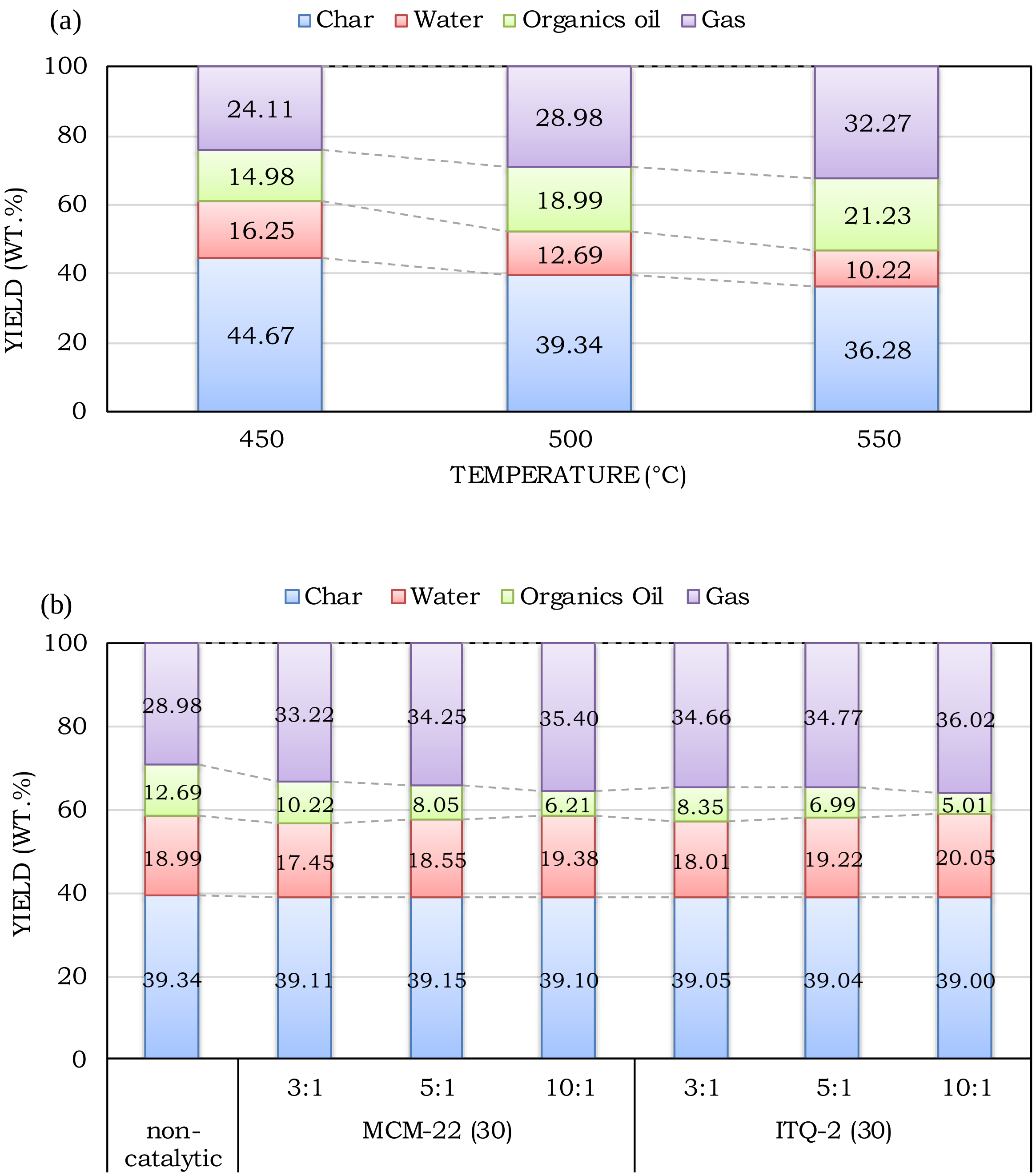

Figure 3: (a) Non-catalytic pyrolysis of *B. Braunii* at various temperatures, (b) catalytic pyrolysis of *B. Braunii*.

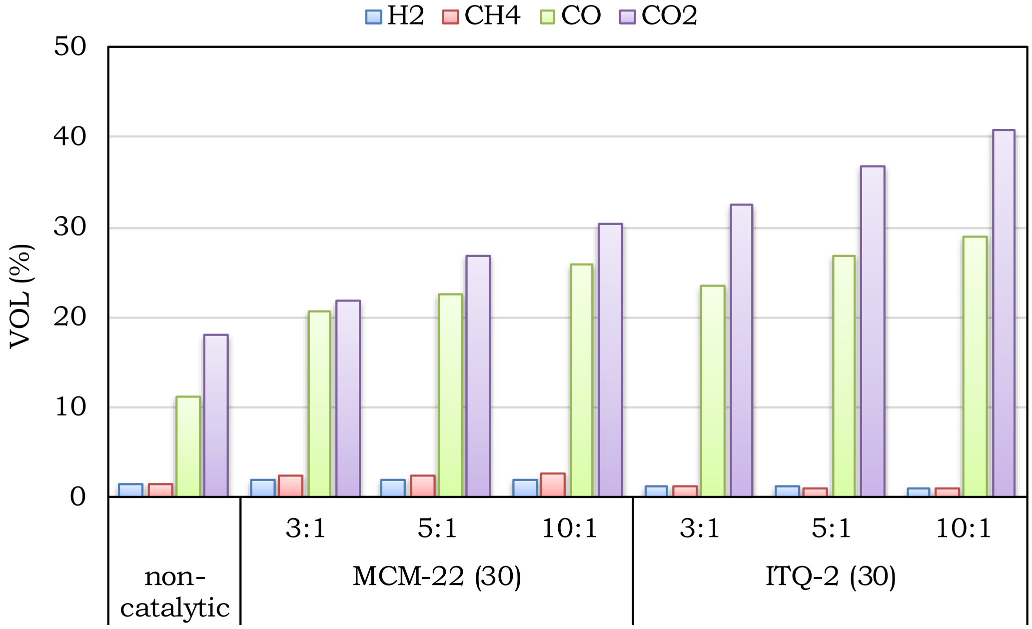

Figure 4: The gas production without catalyst and using catalyst MCM-22(35) and ITQ-2 (35) at different catalyst/biomass ratios

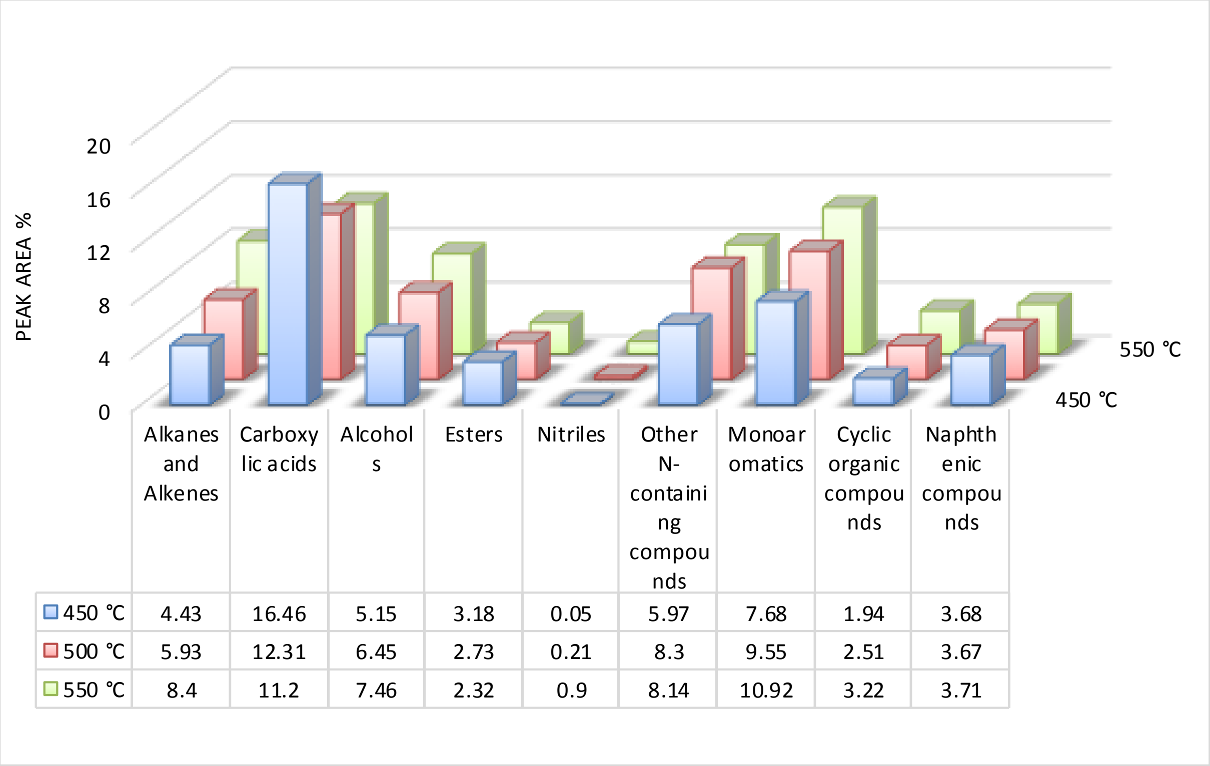

	Alkanes and Alkenes	Carboxylic acids	Alcohols	Esters	Nitriles	Other N-containing compounds	Monoaromatics	Cyclic organic compounds	Naphthenic compounds
🟦 450 ℃	4.43	16.46	5.15	3.18	0.05	5.97	7.68	1.94	3.68
🟥 500 ℃	5.93	12.31	6.45	2.73	0.21	8.3	9.55	2.51	3.67
🟩 550 ℃	8.4	11.2	7.46	2.32	0.9	8.14	10.92	3.22	3.71

Figure 5: Main chemical compounds (area %) present in non-catalytic pyrolysis of *B. braunii* at different pyrolysis process temperatures

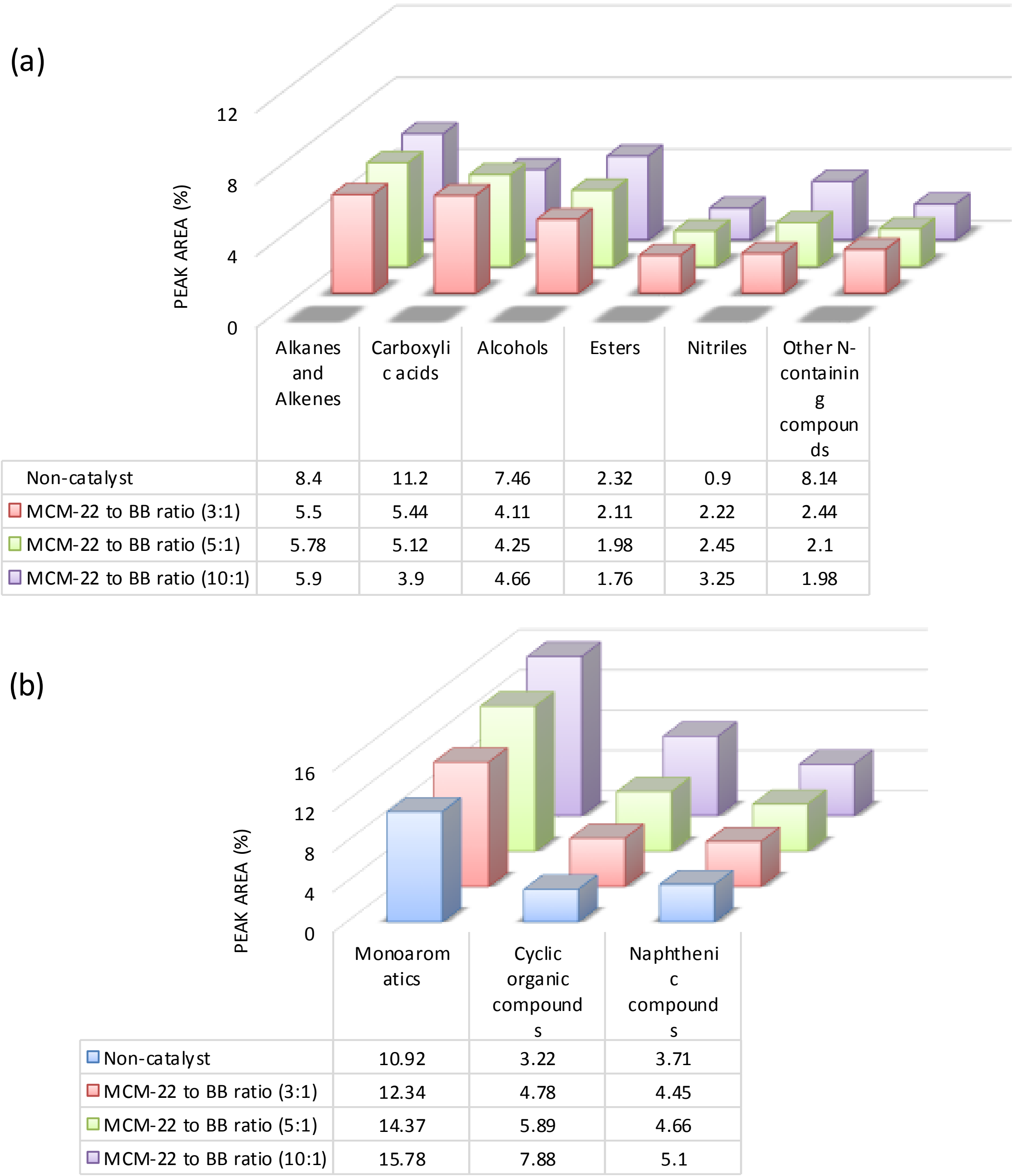

	Alkanes and Alkenes	Carboxylic acids	Alcohols	Esters	Nitriles	Other N-containing compounds
Non-catalyst	8.4	11.2	7.46	2.32	0.9	8.14
🟥 MCM-22 to BB ratio (3:1)	5.5	5.44	4.11	2.11	2.22	2.44
🟩 MCM-22 to BB ratio (5:1)	5.78	5.12	4.25	1.98	2.45	2.1
🟪 MCM-22 to BB ratio (10:1)	5.9	3.9	4.66	1.76	3.25	1.98

	Monoaromatics	Cyclic organic compounds	Naphthenic compounds
🟦 Non-catalyst	10.92	3.22	3.71
🟥 MCM-22 to BB ratio (3:1)	12.34	4.78	4.45
🟩 MCM-22 to BB ratio (5:1)	14.37	5.89	4.66
🟪 MCM-22 to BB ratio (10:1)	15.78	7.88	5.1

Figure 6: (a) Chemical compounds produced in non-catalytic and catalytic (layered zeolites) fast pyrolysis of *B. braunii* at 550 °C (b) Monoaromatics and naphthenic compounds produced over layered zeolite as a function of catalyst/biomass ratios.

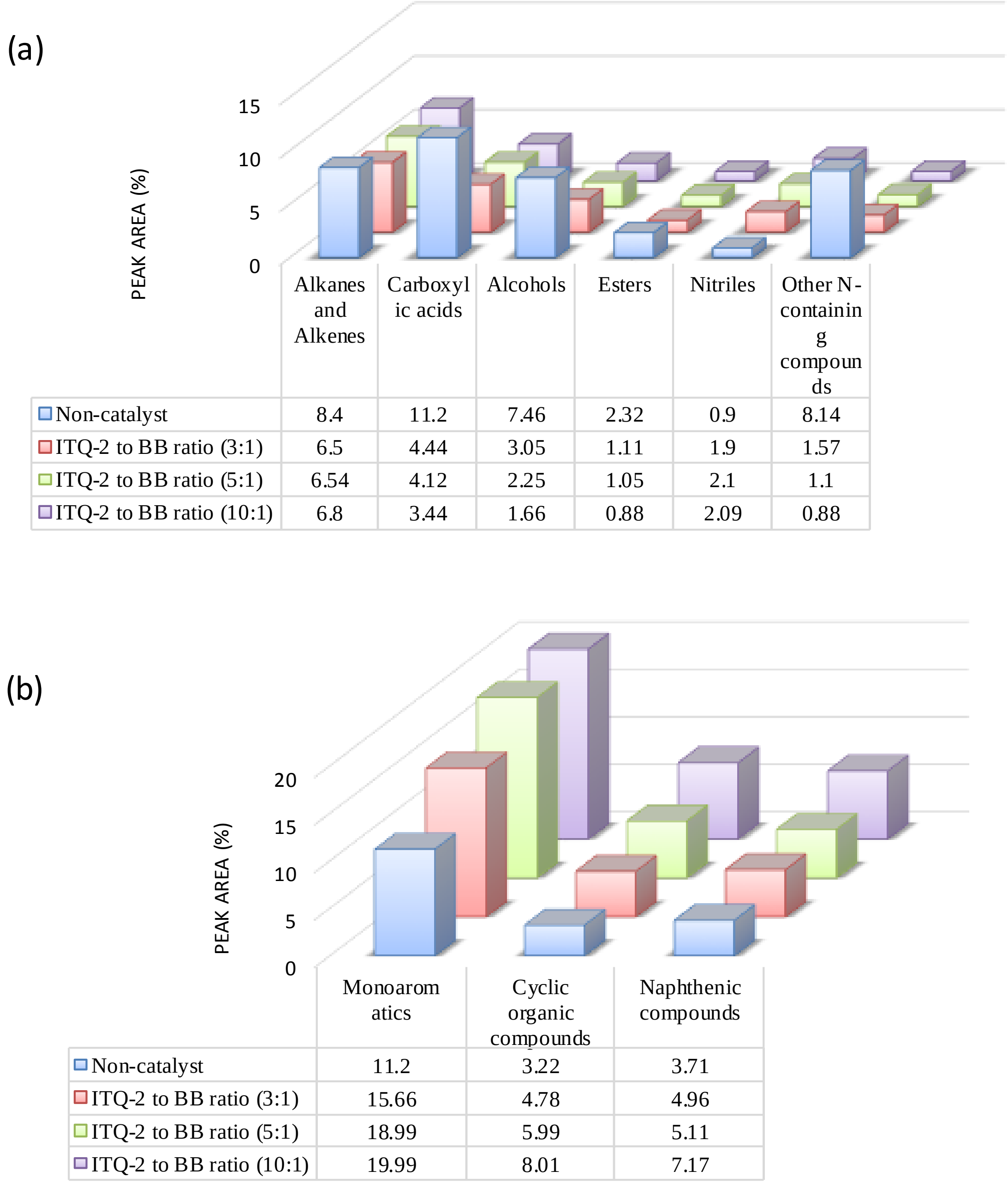

	Alkanes and Alkenes	Carboxylic acids	Alcohols	Esters	Nitriles	Other N-containing compounds
🟦 Non-catalyst	8.4	11.2	7.46	2.32	0.9	8.14
🟥 ITQ-2 to BB ratio (3:1)	6.5	4.44	3.05	1.11	1.9	1.57
🟩 ITQ-2 to BB ratio (5:1)	6.54	4.12	2.25	1.05	2.1	1.1
🟪 ITQ-2 to BB ratio (10:1)	6.8	3.44	1.66	0.88	2.09	0.88

	Monoaromatics	Cyclic organic compounds	Naphthenic compounds
🟦 Non-catalyst	11.2	3.22	3.71
🟥 ITQ-2 to BB ratio (3:1)	15.66	4.78	4.96
🟩 ITQ-2 to BB ratio (5:1)	18.99	5.99	5.11
🟪 ITQ-2 to BB ratio (10:1)	19.99	8.01	7.17

Figure 7: (a) various chemical compounds produced in non-catalytic and catalytic (delaminated zeolites) fast pyrolysis of *B. braunii* at 550 °C (b) Monoaromtics and naphthenic compounds produced over delaminated zeolite as a function of catalyst/biomass ratios.

Table 1: Characteristics of BB

Sample	Proximate analysis (wt.%, db[1])				Ultimate analysis (wt.%, daf[2])				Chemical Composition (wt.%, daf)			Higher heating value
	Moisture	Ash	Volatiles	Fixed Carbon	Carbon	Hydrogen	Nitrogen	Oxygen	Carbohydrates	Protein	Lipids	MJ/kg
B. Braunii	3.5	2.4	76.1	17.9	51.5	8.9	7.5	31.9	24.39	34	20.2	21.5
Spirulina [18]	6.7	7.8	73.1	13.7	48	7.3	10	27	6.7	68.7	14.4	23
Nannochloropsis sp. [19]	3.1	8.9	-	-	49.2	7.2	6.2	32.3	12.4	36.4	27.8	20.5
Scenedesmus dimorphus [20]	0.08	17.3	51.4	31.1	52.6	6.2	8.7	31.9	22.9	53.1	10.2	19
B. Braunii [21]	3.4	2.5	-	-	68.5	9.7	3.8	18	-	-	-	-

[1] Db, dry basis

[2] Daf, dry ash free basis